Performance Model for a Lossless Edge Node of OBS Networks

Guoqiang Hu
Institute of Communication Networks and Computer Engineering
University of Stuttgart, Pfaffenwaldring 47, 70569 Stuttgart, Germany
Email: hu@ikr.uni-stuttgart.de

Abstract

In this paper, the performance model for a lossless OBS edge node is built with respect to the queueing performance of the transmission buffer. In contrast to the shaping effect of the burst assembly in the bufferless edge node, in a lossless edge node the "burstifying" effect of the assembly is more dominant and leads to a worse queueing performance in the transmission buffer. We analyze the traffic characteristic by means of the variance process and identify that there exists a negative correlation structure in the assembled burst traffic in the small time scale, which resembles that of a CBR flow. Through the analysis of the relevant time scale, it is found that this small time scale traffic behavior dominates the queueing performance in most cases and the performance of burst transmission buffer can be well estimated by a corresponding ND/D/1 model. In the case of the self-similar input traffic with large peakness and at a high system load, the tail behavior of large queue length becomes much worse and can be estimated by a Fractional Brownian Motion (FBM) model considering the large time scale traffic behavior. Our performance model provides a simple but accurate analytical method for the performance evaluation and system design.

1 Introduction

In the development of the next-generation optical networks, Optical Burst Switching (OBS) [1, 2] was proposed as a promising IP-over-WDM solution that has a prospective implementation feasibility in the near future. In OBS networks, optical burst units of large size are applied to transport the user data so as to alleviate the per-hop switching overhead and allow for a feasible implementation of the electrical Switching Control Unit (SCU) in the core node. Consequently, in the OBS ingress edge nodes, the burst assembly procedure is necessary to encapsulate the client IP traffic into the optical bursts. The introduction of the burst assembly brings new network performance phenomenon which has aroused lots of research interests.

1.1 Related Work and Motivation

The impact of the burst assembly on the traffic characteristic was studied in [3–5] with respect to the marginal distribution of the burst size and inter-departure time of the assembled bursts.

As the data traffic has a high variability and shows the self-similarity or Long Range Dependence (LRD) [6], the influence of the assembly procedure on the traffic LRD was inspected in [7–10]. Generally, it was shown that the degree of LRD cannot be suppressed by the assembly procedure. However, the burst assembly do have a "shaping effect" on the passing traffic in the sense that it reduces the variability in the inter-departure time of the assembled bursts. This can lead to a better burst loss performance, which was verified by the performance analysis in [11, 12] based on the bufferless model. Especially, it was shown in [11] that the LRD, as a large time scale traffic behavior, has little influence on the loss performance and the burst loss probability is bounded by the Erlang-B formula.

As the edge node is mainly an electrical device, electrical memory components can be deployed to reduce the local burst loss to a very small magnitude. In this case, the queueing delay turns out to be an important performance issue. In [13], the performance of a lossless edge node was studied with simulation, providing an empirical insight into the fundamental system behavior. To the best of our knowledge, analytical performance model for lossless OBS edge node is still missing for general performance estimation and system design. This motivates the contribution of this paper.

1.2 Model, Method and Structure

In this paper, the queueing performance of a lossless edge node will be closely observed. In the system model (Fig. 1), incoming IP packets are classified according to their targeted egress node and QoS class and collected in the assembly queues of corresponding Forwarding Equivalent Class (FEC). Assembled burst traffic is multiplexed into an unbounded transmission buffer where they are scheduled onto the wavelength channel with the FIFO discipline. Here, the offset time for the burst transmission is not considered. Note that if constant offset time is applied, it just introduces an additional constant delay in the burst transmission and therefore can be neglected in the model for statistical queueing analysis.

In principle, multiple channels can share the transmission buffer here to achieve an optimal performance. However, this requires the bandwidth of the memory device to be up to the sum of the channel rate and makes the hardware design utmost challenging. More feasible system design can apply separate transmission buffers with each of them dedicated to one wavelength channel. In this way, the required bandwidth of the memory device is equal to the single channel rate. In this work, we will focus on the system in which the transmission buffer is equipped with a single channel.

As the performance measure, the queue length tail probability (or CCDF function) of $P\{Q > x\}$ is observed for the transmission buffer. Let W denote the queueing delay. Delay performance $P\{W > w\}$ can be approximately derived through the relation $P\{Q > x\} \approx P\{W > x/C\}$, where C is the channel rate.

Due to the traffic multiplexing at the input of the transmission buffer, the traffic characteristic obtained for single assembled burst flow with respect to the inter-burst arrival time [3–5] cannot be directly applied for the performance evaluation. In this paper, we will derive the performance model based on the analysis of the variance process of the aggregated assembled burst process. The variance process $\mathrm{VAR}[A_t]$ is defined as the variance of the random variable A_t where A_t denotes the amount of traffic arrival in an arbitrary time interval of t. The variance process can not only characterize the variability of the traffic arrival [14], but also reflect the correlation structure in the multiple time scales. This makes $\mathrm{VAR}[A_t]$ very "informative" for performance evaluation.

Aggregated traffic generally shows different features at different time scales. In the queueing analysis, it is important to identify which time scale is most relevant for the concerned queueing phenomenon, so that tractable queueing analysis can be carried out by focusing on the traffic behavior in that relevant time scale [15]. For single server queue with Gaussian input process A_t, the queue length tail probability $P\{Q > x\}$ has the relevant time scale $\tau_x = t$ with t maximizing the following measure [15, 16]:

$$\frac{\mathrm{VAR}[A_t]}{(x + t(C - m))^2} \tag{1}$$

Here C is the constant service rate of the single server and m denotes the mean traffic rate. This relation states that the relevant time scale is the period over which the event $\{Q > x\}$ is most likely to occur.

In this paper, it is found that under quite general system scenarios the relevant time scale for the tail probability in the transmission buffer is located on the small time scale, on which the variance process of an individual assembled burst flow resembles that of a Constant Bit Rate (CBR) flow. As a result, the ND/D/1 performance model can be applied to estimate the queueing performance of the transmission buffer. Only in the case of LRD traffic with high peakness and at a high system load, a heavy-tailed queueing performance appears, which can be analyzed based on the LRD property. Above analytical results are verified by the simulation.

This paper is structured as follows. In Section 2 the system model and traffic models will be introduced. In Section 3, the "burstifying" effect of the assembly on the queueing performance will be demonstrated and the worst case assembly scenario is illuminated. In Section 4, we characterize the variance process of the assembled burst traffic under the worst case assembly. In Section 5, the relevant time scale is analyzed based on the variance process of the aggregated traffic and the performance model for the transmission buffer is specified. Simulation results are presented to verify the analytical estimation. In Section 6, the conclusion and outlook are given.

2 System Parameters and Traffic Models

We look at the homogeneous system scenario in the edge node where the assembly control parameters and the traffic parameters are identical for all N FECs. N stands for the number of FECs. FEC traffic flows are independent of each other. The transmission capacity of the wavelength channel is fixed to 10Gbps.

In the observed system model, the burst assembly is controlled by two parameters: maximal burst size S_{max} and timeout period T_{timer} [8]. With the assembly control it is assured that the size of the optical burst is not larger than S_{max} and the packet delay in the assembly buffer is bounded by T_{timer}. While S_{max} is very dependent on the implementation feasibility (e.g. dimensioning of SCU, FDL in the core nodes), T_{timer} is determined by the allocated delay budget in the edge node.

Modelling of IP traffic is still an ongoing research issue. While the IP traffic was proved to show LRD [6] in the large time scale, it was also realized [17] that in the small-time scale the backbone IP traffic shows the Poisson-alike behavior due to the traffic aggregation. In this work, both Poisson traffic model and LRD traffic model are adopted.

In the Poisson traffic model, the packet arrival follows the Poisson process and the packet length L is independently identically distributed (iid) with P$\{L = 40$ bytes$\} = 0.49$, P$\{L = 576$ bytes$\} = 0.17$, P$\{L = 1500$ bytes$\} = 0.17$ and P$\{L =$ x bytes$\} = 0.17/535$ for $41 \leq x \leq 575$ [18]. As a LRD model, M/Pareto process [19] is used. With this model, data sessions are generated

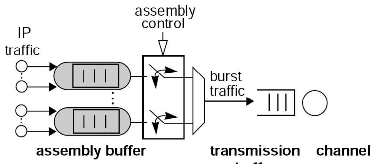

Figure 1: System model of an OBS edge node

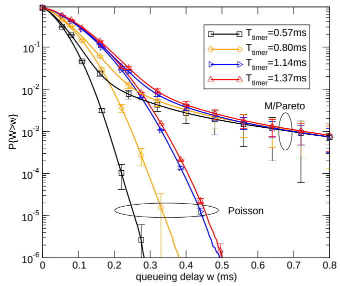

Figure 2: Delay CCDF with respect to different T_{timer}

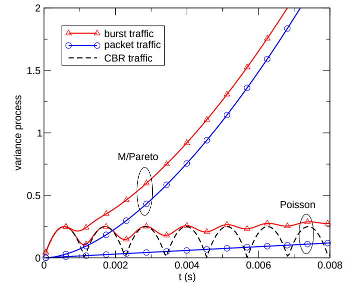

Figure 3: Variance process with respect to time scale t

according to Poisson process. The size of a session follows the Pareto distribution with a mean value of μ and the shaping parameter α. In each data session, the data is sent at a constant rate of R. The rate R can be regarded as the link capacity of the access link on which each data session is transmitted. In this sense, the M/Pareto process is an inherent model for the aggregated traffic. The traffic generated by M/Pareto process shows uncorrelation in the small time scale and LRD characteristic in the large time scale, fitting the measured multi-timescale characteristic of the backbone IP traffic very well. The degree of LRD is characterized by the Hurst parameter H determined by $H = (3 - \alpha)/2$. In the presentation of the numerical results in the following sections, the setting of $\alpha = 1.4$, $\mu = 10$KBytes will be used uniformly for the M/Pareto model.

3 Assembly as a "Burstifier"

Significant influence of the burst assembly procedure on the traffic characteristics lies in two aspects. On one side, the variability of the assembled burst inter-departure time is smaller than that of the packet interarrival time. On the other hand, the burst size is generally much larger than the IP packet size. In a bufferless (pure loss) model, the burst loss probability is relative insensitive to the burst size, so the more evenly distributed burst arrival leads to an improved performance.

In a lossless edge node, however, both effects are relevant. In particular, the large burst size means large instantaneous jump in the arrival process of the traffic amount (in byte) which is detrimental for the queueing performance. In [14] it is heuristically shown that the transform of a packet arrival process by aggregating packets into super-frames results in a more variable traffic process. This indicates that burst assembly can lead to a worse performance in the burst transmission buffer.

Above intuitive estimation is verified by our extensive simulation study for both Poison and M/Pareto traffic model. Representative results are shown in Fig. 2 illustrating the CCDF of the queueing delay in the transmission buffer at a system load of 0.9. $N = 20$, $S_{max}=$ 64KBytes and T_{timer} is set to different values respectively. Especially for the M/Pareto model, the access link rate here is $R = 50$Mbps.

It can be seen that with both traffic models the queueing delay continuously increases with the increasing T_{timer} and finally converges to be constant irrespective of the further change of T_{timer}. This is due to the fact that the increase of T_{timer} leads to larger size of the assembled bursts.

However, when the T_{timer} is large enough, the parameter S_{max} dominates the assembly control and the burst size reaches its maximum. Further change of T_{timer} has no more influence.

Special interesting queueing behavior is observed for the M/Pareto traffic. It is seen that queueing delay only gets worse in the range of small w with the increasing T_{timer}. For large w, T_{timer} causes little difference. This is because the burst assembly has little impact on the large time scale characteristic of the passing traffic, which will become clearer in the following sections.

It is seen that the worst queueing performance appears when the parameter S_{max} dominates the assembly control. In addition, it is reasonable to suppose that most of the bursts should reach the size of S_{max} when the system runs at the designed full load. Therefore, we will focus on this worst case assembly scenario in the following sections and the influence of the parameter T_{timer} will be neglected.

4 Variance Process of Assembled Traffic

In this section, the variance process of the assembled burst traffic is analyzed and the traffic statistic on different time scales is inspected.

Let U_t denote the amount (in byte) of IP traffic arrival at the input of an assembly buffer in an arbitrary interval of t. The average traffic rate is ψ. Therefore, the mean value $\mathrm{E}[U_t] = \psi t$. We assume that the IP traffic can be approximated as a fluid flow model and U_t is a Gaussian process with a Probability Density Function (PDF) of $p_t(u)$. V_t stands for the number of burst departures from the assembly buffer in the interval t. The burst inter-departure time is denoted by D.

In case S_{max} dominates the assembly procedure, a departure burst always has the maximal size of S_{max}. Therefore, $\mathrm{E}[V_t] = \mathrm{E}[U_t]/S_{max}$. r_{U_t} denote the residual of the division U_t/S_{max}, i.e., $r_{U_t} = U_t/S_{max} - \lfloor U_t/S_{max} \rfloor$, it can be derived [14]:

$$V_t = \begin{cases} \lfloor U_t/S_{max} \rfloor + 1 & \text{with probability } r_{U_t}, \\ \lfloor U_t/S_{max} \rfloor & \text{with probability } 1 - r_{U_t}. \end{cases} \tag{2}$$

And the variance process $\mathrm{VAR}[V_t]$ is calculated as [14]:

$$\begin{aligned} & \mathrm{E}[{V_t}^2] - \mathrm{E}[V_t]^2 \\ = \; & \int_0^\infty \mathrm{E}[{V_t}^2 | U_t = u] p_t(u) \, \mathrm{d}u - \mathrm{E}[V_t]^2 \\ = \; & \int_0^\infty (r_u(\lfloor \frac{u}{S_{max}} \rfloor + 1)^2 + (1 - r_u)(\lfloor \frac{u}{S_{max}} \rfloor)^2) \\ & \cdot p_t(u) \, \mathrm{d}u - (\frac{\mathrm{E}[U_t]}{S_{max}})^2 \end{aligned} \tag{3}$$

However, a closed form solution for Eq.(3) is hard to obtain due to the floor function in the integral. In the following, we aim to derive the approximate solution to $\mathrm{VAR}[V_t]$ for small and large t.

We note that Eq.(3) can be rewritten as:

$$\int_0^\infty ((\lfloor \frac{u}{S_{max}} \rfloor + r_u)^2 + (r_u - r_u^2)) p_t(u)\,\mathrm{d}u - (\frac{\mathrm{E}[U_t]}{S_{max}})^2$$
$$= \int_0^\infty ((\frac{u}{S_{max}})^2 + (r_u - r_u^2)) \cdot p_t(u)\,\mathrm{d}u - (\frac{\mathrm{E}[U_t]}{S_{max}})^2$$
$$= \int_0^\infty (r_u - r_u^2) \cdot p_t(u)\,\mathrm{d}u + \frac{\mathrm{VAR}[U_t]}{S_{max}^2} \tag{4}$$

Eq.(4) clearly illuminates the relationship between VAR[V_t] and VAR[U_t].

4.1 Small Time Scale Approximation

In the small time scale $t \to 0$, VAR[U_t] is small and the PDF $p_t(u)$ tends to an impulse located at u = E[U_t] = ψt. At the same time, the term VAR[U_t]/S_{max}^2 is small and can be ignored. This leads to the small time scale approximation of VAR[V_t]:

$$\mathrm{VAR}[V_t] \approx (r_u - r_u^2)|_{u=\psi t} \tag{5}$$

Observing $r_{\psi t} = \psi t/S_{max} - \lfloor \psi t/S_{max} \rfloor$ and taking the fact that the mean burst inter-departure time $\mathrm{E}[D] = S_{max}/\psi$, it results in $\eta_t = r_{\psi t} = t/\mathrm{E}[D] - \lfloor t/\mathrm{E}[D] \rfloor$. An alternative to Eq.(5) is:

$$\mathrm{VAR}[V_t] \approx \eta_t - \eta_t^2 \tag{6}$$

It can be shown based on the results in Section III.A of [20] that Eq.(6) is actually the variance process of a CBR flow with a constant inter-arrival time equal to E[D]. This indicates that in the small time scale the variance structure of the assembled burst traffic resembles the pattern of a CBR flow.

4.2 Large Time Scale Approximation

Since $0 \leq r_u < 1$ is a periodic function of u with the period equal to S_{max}, the integration operation in Eq.(4) can be represented by a sum of piecewise integration:

$$\mathrm{VAR}[V_t] - \frac{\mathrm{VAR}[U_t]}{S_{max}^2}$$
$$= \sum_{k=0}^{\infty} \int_0^{S_{max}} (\frac{\zeta}{S_{max}} - (\frac{\zeta}{S_{max}})^2) p_t(kS_{max} + \zeta)\,\mathrm{d}\zeta \tag{7}$$

In the large time scale, both E[U_t] and VAR[U_t] are large and the span of PDF $p_t(u)$ is much greater than S_{max}. Therefore, $p_t(kS_{max} + \zeta) \approx p_t(kS_{max})$ for $0 < \zeta < S_{max}$. Eq.(7) can be approximated as:

$$
\begin{aligned}
& \mathrm{VAR}[V_t] - \frac{\mathrm{VAR}[U_t]}{S_{max}^2} \\
\approx \quad & \sum_{k=0}^{\infty} p_t(kS_{max}) \cdot \int_0^{S_{max}} (\frac{\zeta}{S_{max}} - (\frac{\zeta}{S_{max}})^2)\,\mathrm{d}\zeta \\
= \quad & \sum_{k=0}^{\infty} p_t(kS_{max}) \cdot \frac{S_{max}}{6} \approx \frac{1}{6} \qquad (8)
\end{aligned}
$$

This leads to the large time scale approximation:

$$
\mathrm{VAR}[V_t] \approx \frac{1}{6} + \frac{\mathrm{VAR}[U_t]}{S_{max}^2} \qquad (9)
$$

4.3 Numerical Solution

To have a complete view of the variance structure and verify the small/large time scale approximation, the variance process is studied by solving Eq.(4) numerically and also by simulation. Since the results conform to each other quite well, only the numerical results are shown in this section.

For the computation, the Gaussian PDF $p_t(u)$ is specified by matching its mean and variance to those of the incoming IP traffic. While the mean value is straightforward to determine, the variance of the IP traffic arrival process is dependent on the traffic model. In the case of the Poisson model, the amount of traffic arrival follows the compound Poisson distribution, the variance of which can be got according to the standard probability theory. In the case of M/Pareto model, its variance process is obtained according to the analysis in [19, 21].

In Fig.3, resulting $\mathrm{VAR}[V_t]$ (burst traffic) is plotted together with the related $\mathrm{VAR}[U_t]/S_{max}^2$ (packet traffic). For comparison, the variance process of the corresponding CBR flow (Eq.(6)) is also shown. S_{max}=64KBytes. For both traffic models, the mean IP traffic rate is 450 Mbps. In the M/Pareto model, access link rate $R = 50$Mbps.

It can be seen that in both cases, the variance structure of burst traffic looks like the normalized variance process of the packet traffic incremented by a positive factor. This factor fluctuates periodically in the small time scale and converges to be constant with the increasing time scale. This phenomenon can be exactly explained by the form of the Eq.(4). In the small time scale, $\mathrm{VAR}[V_t]$ is tightly consistent with the variance process of the CBR traffic, which verifies our small time scale approximation. Especially, the decreasing part of the variance structure in the burst traffic and the CBR traffic is an indication of the existence of negative correlation, which is caused by the floor function. In the large time scale, the variance process of the burst traffic and packet traffic tends to be parallel. A closer inspection discovers that the difference between them is about 0.16. This is consistent with the large time scale approximation in Eq.(9).

Noticeable difference between the two models lies in the dramatic increase of $\mathrm{VAR}[V_t]$ with t in the case of M/Pareto model due to the LRD property. As a result, $\mathrm{VAR}[V_t]$ converges faster to the large time scale approximation. In very large time scales, the constant item of 1/6 in Eq.(9) becomes negligible, meaning that the burst assembly has little influence on the large time scale traffic characteristic.

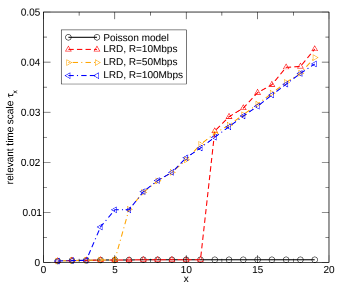

Figure 4: Relevant time scale wrt. normalized queue length x

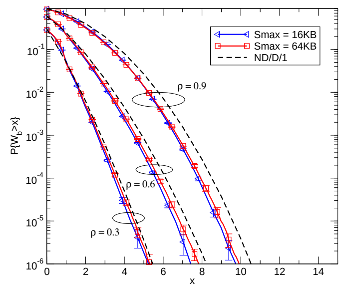

Figure 5: CCDF of normalized queueing delay, Poisson model

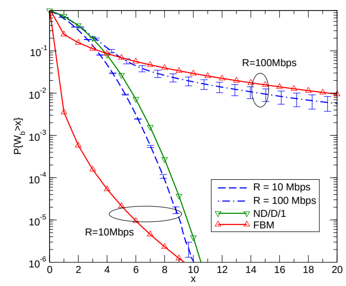

Figure 6: CCDF of normalized queueing delay, M/Pareto model

5 Performance of Transmission Buffer

In this section, the relevant time scale is analyzed based on the variance process of the aggregated burst traffic. It is shown that depending on the location of the relevant time scale, well known ND/D/1 model [20] as well as Fractional Brownian Motion (FBM) model [22] can be used to estimate the performance of the transmission buffer under the worst-case assembly scenario.

5.1 Calculation of Relevant Time Scale

Let M_t represent the variance process of the aggregated burst arrival at the input of the transmission buffer. For the homogeneous scenario and independent FEC flows as stated in Section II, there is $\mathrm{VAR}[M_t] = N \cdot \mathrm{VAR}[V_t]$. By replacing the $\mathrm{VAR}[A_t]$ in Eq.(1) with $\mathrm{VAR}[M_t]$, the relevant time scale τ_x with respect to the queue length tail probability $\mathrm{P}\{Q_b > x\}$ is obtainable by numerical optimization. Note that Q_b is the number of the bursts in the transmission buffer.

In Fig.4 τ_x is shown for both IP traffic models at a system load of 0.9. $N = 20$. It can be seen that in the case of Poisson model, the relevant time scale remains in the small time scale for all values of x. With the M/Pareto model, in the range of small x, τ_x is small, similar to the case of Poisson model. However, with the increasing x, τ_x jumps to the large time scale at a critical value of $x = x_c$, depending on the access link rate R. A large R leads to a small x_c, making τ_x shift to the large time scale even for pretty small x.

5.2 Estimation of the Queueing Performance

As shown in the Section IV, in the small time scale, the variance process of an individual burst departure traffic is analogous to a CBR flow whose arrival period is equal to the mean burst departure time $\mathrm{E}[D]$. As a result, the aggregated burst traffic behaves like the multiplexing of N CBR flows in the small time scale. This implies that the ND/D/1 model can be applied for performance estimation as long as the respective τ_x is located in the small time scale.

Since τ_x remains low in the case of Poisson model, according to ND/D/1 model [20] $P\{Q_b > x\}$ is estimated by:

$$\sum_{x<k\leq N} \binom{N}{k} (\frac{k-x}{\mathrm{E}[D]})^k (1-\frac{k-x}{\mathrm{E}[D]})^{N-k} (\frac{\mathrm{E}[D]-N+x}{\mathrm{E}[D]-k+x}) \tag{10}$$

Let W_b denote the queueing delay normalized by one burst transmission time on the wavelength channel. The delay performance can be analytically obtained by $P\{W_b > x\} \approx P\{Q_b > x\}$. In Fig.5, the goodness of the estimation of W_b is shown by comparing with the simulation results. Different system loads (0.3, 0.6, 0.9) and different S_{max} (16KBytes, 64KBytes) are inspected. $N = 20$. It can be seen that the ND/D/1 analytical model really serves as a tight approximation under every scenario.

When the M/Pareto model is concerned, Eq.(10) is still applicable in the range of small x, because τ_x is also small. However, for large x τ_x increases very fast. So the large time scale traffic behavior has more influence on the queueing performance. In the large time scale, the M/Pareto process converges to FBM process [19]. Using the queueing analysis for FBM process [21, 22], it is obtained for large x:

$$P\{Q_b > x\} \approx \exp(-\frac{(C-m)^{2H} x^{2-2H}}{2H^{2H}(1-H)^{2-2H} \cdot a \cdot m}) \tag{11}$$

Here C denotes the channel transmission rate and m is the total traffic rate at the transmission buffer. H is the Hurst parameter and a is calculated as [21]:

$$a = \frac{R^{2H-1} \cdot (\frac{2-2H}{3-2H} \cdot \mu)^{2-2H}}{(3-2H) \cdot (2H-1) \cdot H} \tag{12}$$

R is the access link rate and μ is the mean session size defined in Section II. Note that the unit of the parameter C, m, R, μ should be correspondingly adapted according to the unit of Q_b.

Based on Eq.(10) and Eq.(11), $P\{W_b > x\}$ for M/Pareto traffic can be derived for small and large x respectively. The results are plotted in Fig.6 in comparison with the simulation. The system load is 0.9. It is seen that for M/Pareto traffic with small access link rate R (10Mbps), the performance is still well estimated by the ND/D/1 model over the wide range of x. This is in consistency with its τ_x plotted in Fig.4. For large R (100Mbps), in the range of small x, the CCDF curve follows the analytical result from the ND/D/1 model. For large x, the FBM model estimates the performance very well.

It is worth pointing out, although the determination of the τ_x needs the numerical optimization, the queueing performance can be directly estimated with the closed form solutions of Eq.(10) and Eq.(11). In addition, due to the continuity of the general tail probability of the queueing delay, the critical value x_c for M/Pareto traffic can be actually estimated from the intersection point of the curves estimated by the ND/D/1 model and FBM model as shown in Fig.6.

5.3 Discussion

Our performance analysis shows that the detrimental effect of the LRD traffic characteristic on the queueing performance can be eliminated by keeping a large aggregation level of the traffic.

That is, keeping the access link rate of individual traffic sources relative small in comparison to the mean rate of the aggregated traffic, or equivalently (in the case of a fixed load) in comparison to the channel capacity in the backbone link. This helps drive the edge node operating in a good performance region, where it resembles a ND/D/1 model.

By modelling with a ND/D/1 system, it is realized that the maximal burst size S_{max} is a decisive parameter for the queueing performance under specified system load and the number of FECs N. For example, at the load of 0.9 with $N = 20$, it is shown in Fig.5 that $P\{W_b > 11\} < 10^{-6}$. On a 10Gbps channel, this leads to an absolute queueing delay $P\{W > 0.14\text{ms}\} < 10^{-6}$ for a small S_{max}=16KBytes. In comparison to the T_{timer} which is generally in the range of several millisecond depending on the delay budget specification, the queueing delay is one magnitude smaller and can be neglected, even at such a high load (90%). This also justifies the application of FIFO buffer here since more advanced scheduling can not bring much improvement anyway despite of the increased complexity. However, if a large $S_{max} = 128$KBytes is defined, it means $P\{W > 1.13\text{ms}\} < 10^{-6}$. The queueing delay is then comparable to T_{timer} and must be considered. In that case, it can be necessary to adopt advanced scheduling procedures to differentiate and guarantee the quality of service.

6 Conclusion and Outlook

In this paper, the influence of the burst assembly on the traffic characteristic and system performance in a lossless edge node is inspected with Poisson and LRD IP traffic. It is found that the burst assembly leads to a worse system performance due to the increased size of the data transmission unit (burst). The worst case occurs when the size parameter S_{max} dominates the assembly procedure and all bursts have the maximal size. The variance process of the burst traffic is analyzed especially for the small and large time scale under the worst case assembly. It is figured out that the assembly procedure brings a negative correlation structure in the small time scale that resembles a CBR flow. In the large time scale, the burst assembly has only little impact on the variance process of the traffic. Based on the analysis of the relevant time scale, we show the queueing performance of the burst transmission buffer can be conveniently estimated through approximating the system by ND/D/1 or FBM model. Both models are simple and accurate, which can serve as parsimonious performance models for the delay estimation as well as buffer dimensioning in the edge node.

In this work, no offset time in the burst transmission is considered in the system model. The OBS scheme with constant offset time can still be covered by the proposed performance model by treating the offset time as a constant extra delay. However, in case of variable offset time the system behavior will be quite different. This issue will be the subject of future research.

Acknowledgments

This work was supported in part by the IST-FP6 Network of Excellence (NoE) e-Photon/ONe and e-Photon/ONe+.

The author would like to thank Dr. Javier Aracil and Dipl.-Ing. MSCS. Christoph Gauger for the constructive discussions and valuable comments, and Mr. Baizhan Kanafin for his preparation and analysis of the simulation results.

References

[1] C. Qiao and M. Yoo, “Choices, features and issues in optical burst switching,” *Optical Networking Magazine*, vol. 1, no. 2, 2000.

[2] C. Qiao, M. Yoo, and S. Dixit, “Optical burst switching for service differentiation in the next-generation optical internet,” *IEEE Communications Magazine*, vol. 39, no. 2, 2001.

[3] K. Laevens, “Traffic characteristics inside optical burst switched networks,” in *Proceeding of the SPIE OptiCom*, 2002.

[4] X. Yu, Y. Chen, and C. Qiao, “A study of traffic statistics of assembled burst traffic in optical burst switched networks,” in *SPIE OptiCom*, 2002.

[5] M. de Vega Rodrigo and J. Goetz, “An analytical study of optical burst switching aggregation strategies,” in *Proceedings of the Third International Workshop on Optical Burst Switching (WOBS)*, 2004.

[6] W. Willinger, V. Paxson, R. H. Riedi, and M. S. Taqqu, *Long-range dependence: theory and applications.* Birkhauser, 2002.

[7] A. Ge, F. Callegati, and L. S. Tamil, “On optical burst switching and self-similar traffic,” *IEEE Communications Letter*, vol. 4, no. 3, 2000.

[8] F. Xue and S. J. B. Yoo, “Self-similar traffic shaping at the edge router in optical packet switched networks,” in *IEEE ICC*, 2002.

[9] G. Hu, K. Dolzer, and C. M. Gauger, “Does burst assembly really reduce self-similarity?” in *OFC*, 2003.

[10] X. Yu, J. Li, X. Cao, Y. Chen, and C. Qiao, “Traffic statistics and performance evaluation in optical burst switched networks,” *Journal of Lightwave Technology*, vol. 22, no. 12, 2004.

[11] M. Izal and J. Aracil, “On the influence of self-similarity on optical burst switching traffic,” in *IEEE Globecom*, 2002.

[12] X. Yu, Y. Chen, and C. Qiao, “Performance evaluation of optical burst switching with assembled burst traffic input,” in *IEEE Globecom*, 2002.

[13] R. Rajaduray, S. Ovadia, and D. Blumenthal, “Analysis of an edge router for span-constrained optical burst switched (OBS) networks,” *IEEE Journal on Lighwave Technology*, vol. 22, no. 11, 2004.

[14] T. Bonald, A. Proutiere, and J. Roberts, “Statistical performance guarantees for streaming flows using expedited forwarding,” in *INFOCOM*, 2001.

[15] A. Neidhardt and J. Wang, “The concept of relevant time scales and its application to queueing analysis of self-similar trafic,” in *Proceedings of SIGMETRICS ’98/PERFORMANCE ’98*, 1998.

[16] J. Choe and N. Shroff, “A central-limit-theorem-based approach for analyzing queue behavior in high-speed networks,” *IEEE/ACM Transactions on Networking*, vol. 6, no. 5, 1998.

[17] Z. Zhang, V. J. Ribeiro, S. Moon, and C. Diot, "Small-time scaling behaviors of internet backbone traffic: an empirical study," in *IEEE INFOCOM*, 2003.

[18] k claffy, G. Miller, and K. Thompson, "The nature of the beast: recent traffic measurements from an internet backbone," in *International Networking Conference (INET)*, 1998.

[19] T. D. Neame, M. Zukerman, and R. G. Addie, "Modeling broadband traffic streams," in *IEEE Globecom*, 1999.

[20] I. Norros, J. Roberts, A. Simonian, and J. Virtamo, "The superposition of variable bit rate sources in an ATM multiplexer," *IEEE Journal of Selected Areas in Communications*, vol. 9, no. 3, 1991.

[21] S. Bodamer and J. Charzinski, "Evaluation of effective bandwidth schemes for self-similar traffic," in *13th ITC Specialist Seminar on IP Traffic Measurement, Modeling and Management*, 2000.

[22] I. Norros, "On the use of fractional brownian motion in the theory of connectionless networks," *IEEE Journal of Selected Areas in Communications*, vol. 13, no. 6, 1995.